Understanding the Necessity and Economic Benefits of Lockdown Measures to Contain COVID-19

Zhengqiu Zhu, Chuan Ai, Hailiang Chen, Bin Chen, Wei Duan, Xiaogang Qiu, Xin Lu, Ming He, Zhiming Zhao, *Senior Member, IEEE*, and Zhong Liu

***Abstract*— Since the outbreak of the coronavirus disease 2019 (COVID-19), the issue of how to maintain economic development while containing the epidemic has become a significant concern for decision-makers. Though lockdown measures are verified to be very effective in containing the epidemic, its economic costs and other influences have not been fully explored. As a result, decision-makers in many countries are still hesitant to include the lockdown measure in an intervention strategy in response to COVID-19. To address this issue, we propose a universal computational experiment approach for policy evaluation and adjustment based on the Artificial societies, Computational experiments, Parallel execution (ACP) concept. First, we innovatively construct a model via observable CO_2 emissions, which is able to estimate the economic costs affected by nonpharmaceutical interventions. Furthermore, based on the population movement data, a risk source model is proposed to estimate the local transmission risk for any prefectures outside the epicenter. Finally, we integrate the data models in a high-resolution agent-based artificial society and carry out large-scale computational experiments supported by the Tianhe supercomputer. Policy adjustments and evaluations are carried out in four cities: Wenzhou, Guangzhou, Beijing, and Wuhan. Our research findings show important implications for policy-making: 1) the local transmission of a city can be almost contained if lockdowns are adopted immediately when the risk index is larger than 1.645, 1.960, or 2.576 at the 90%, 95%, or 99% confidence interval, respectively; 2) if lockdowns are required, in-advance lockdown measures facilitate mitigation efficacy and reduce economic loss; and 3) lockdowns lasting for 7–14 days in a prefecture would be effective in controlling the spread of the epidemic. The duration of the measure should be prolonged with the increment of the initial transmission risk.**

***Index Terms*— Coronavirus disease 2019 (COVID-19), high-resolution agent-based artificial society, lockdown measures, policy-making, risk source model.**

I. Introduction

SINCE December 2019, an increasing number of cases of the coronavirus disease 2019 (COVID-19) caused by severe acute respiratory syndrome coronavirus 2 (SARS-CoV-2) have been first identified in Wuhan, the capital of Hubei province. The outbreak of COVID-19 was then rapidly followed by the rest prefectures in mainland China [1]–[3]. Due to the intense quarantine and lockdown measures adopted by all prefectures during the Spring Festival, the epidemic was under control to a large extent by the end of March 2020, however, with a huge cost. Despite the unprecedented mitigation measures adopted by China, COVID-19 was not completely contained, and the contagion was soon identified in other countries. Notably, the emergence of various variants of COVID-19 (e.g., Delta and Omicron) has made the prevention and control of the epidemic more difficult [4].

In response, governments in different countries have adopted various intervention strategies to struggle with the epidemic. For instance, many previous studies [5]–[9] have made exploratory works on predicting the spread of the epidemic and its evolution within their jurisdictions. To address the efficacy of various interventions, some researchers [10]–[12] explored the relationship between the strength of the measures taken and the effectiveness of COVID-19 containment. As pointed out in [5], stringent quarantine, case isolation, and social distance measures were evidenced to be the most effective measures other than the application of COVID-19 vaccines. Although China has limited a larger outbreak and spread of the disease in a relatively short period, its potential high economic costs have stirred a global debate on whether such stringent measures were necessary at the initial stage of the pandemic and on how to relax them while avoiding huge epidemic peaks in the future. The doubt still haunts many researchers and policy-makers, and remains to be solved.

The current actions adopted are mainly hampered by two important challenges: 1) it is difficult to predict the impacts of intervention strategies (e.g., limiting economic activities)

Manuscript received 10 March 2022; revised 10 July 2022 and 14 July 2022; accepted 25 July 2022. This work was supported in part by the National Natural Science Foundation of China under Grant 62173337, Grant 21808181, Grant 72071207, Grant 72025405, Grant 71790615, Grant 91846301, and Grant 72088101; in part by the Shenzhen Basic Research Project for Development of Science and Technology under Grant JCYJ20200109141218676 and Grant 202008291726500001; in part by the Innovation Team Project of Colleges in Guangdong Province under Grant 2020KCXTD040; and in part by the Humanity and Social Science Youth Foundation of the Ministry of Education of China under Grant 19YJCZH073. *(Zhengqiu Zhu and Chuan Ai contributed equally to this work.) (Corresponding authors: Bin Chen; Wei Duan.)*

Zhengqiu Zhu, Chuan Ai, Hailiang Chen, Bin Chen, Wei Duan, Xiaogang Qiu, Xin Lu, and Zhong Liu are with the College of Systems Engineering, National University of Defense Technology, Changsha, Hunan 410073, China (e-mail: zhuzhengqiu12@nudt.edu.cn; aichuan@nudt.edu.cn; chenhailiang@nudt.edu.cn; nudtcb9372@gmail.com; duanwei@nudt.edu.cn; michael.qiu@139.com; xin.lu@flowminder.org; phillipliu@263.net).

Ming He is with the Command and Control Engineering College, Peoples Liberation Army Engineering University, Nanjing, Jiangsu 210001, China (e-mail: paper-review@126.com).

Zhiming Zhao is with the Research Group of Multi-Scale Networked Systems, University of Amsterdam (UvA), 1012 WX Amsterdam, The Netherlands (e-mail: z.zhao@uva.nl).

This article has supplementary downloadable material available at https://doi.org/10.1109/TCSS.2022.3194639, provided by the authors.

Digital Object Identifier 10.1109/TCSS.2022.3194639

on the pandemic and the economic losses (and their relations) and 2) it is not clear how population movements and other demographic factors can influence the epidemic transmission. Thus, it is difficult to evaluate the containment effects of intervention strategies on COVID-19 originated from a major epicenter or multiple epicenters. In this context, we propose a universal computational experiment approach based on the Artificial societies, Computational experiments, Parallel execution (ACP) concept [13] to evaluate the mitigation efficacy and economic costs of any intervention strategies. The proposed approach employs a customized high-resolution agent-based artificial society with a derived risk source model and an economic cost model based on real-world datasets.

As an important factor in the economy both for production and consumption, carbon dioxide (CO_2) emissions are known to be directly linked to the economic growth [14]. Also, it usually takes a relatively long time for the authorities to acquire and publish economy- and pandemic-related data. Thus, we leverage the CO_2 emissions data running in a real-time mode to estimate the economic development data in this article. Supported by previous efforts [15]–[18] made to quantify the impact of the pandemic on CO_2 emissions, we investigate the feasibility of using CO_2 emissions data as a bridge to estimate the economic costs of intervention strategies. Here, we answer the first question of what would have been the number of COVID-19 cases and the economic costs if the city governors have taken stronger (or weaker) measures or if these measures have been taken earlier (or later).

We extract the outbound flows from Wuhan through nationwide mobile-phone data and analyze the relations between the number of outbound flows and COVID-19 cumulative incidence in that locale [19], [20]. By computing the relative difference between the predicted number of cumulative cases (estimation based on outbound flows to any prefectures) and the official reported COVID-19 cases, we develop a dynamic risk source model to operationalize the risk emanating from an epidemic center. Through assessing the risk index yielded by the model, the regions with a high risk of community transmission of COVID-19 at an early stage can be identified. Here, we answer the second question of what would have been the epidemic in prefectures outside the epicenter if the population movements from the epidemic center to other locales are considered.

We also construct a high-resolution agent-based artificial society for target cities (e.g., Wenzhou, Guangzhou, Beijing, and Wuhan) based on four main models: the environment model, the agent model, the contact behavior model, and the disease spread model [21]. We adopt the agent-based model and the network model to describe the relations among different agent clusters in light of the advantages of these models in tracing the fine-grained effect of intervention strategies under diverse epidemic settings. The models used in the artificial society are calibrated to the main features of COVID-19. The sensitivity analysis also reveals that key epidemiological outputs of our model (e.g., the basic reproductive number and the generation period) are robust to uncertainty that existed in the input parameters.

In this study, by integrating the data models with high-resolution agent-based artificial society, we unleash the full potential of the computational experiment approach in evaluating and tailoring interventions to realize the tradeoffs between economic development and epidemic containment, especially in assessing the necessity and economic benefits of lockdown measures. The contribution of this work can be summarized as follows.

1) We propose a universal computational experiment approach and high-resolution artificial society for policy evaluation and adjustment in response to COVID-19. Notably, our computational experiment approach is suitable for evaluations of any intervention strategies. Moreover, the constructed artificial society is applicable at different scales for simulation and assessment of the pandemic. That is to say, the artificial society can be easily extended to microlevel (e.g., in a classroom), regional level (e.g., in a city), and macrolevel (e.g., in a country).
2) Different from the previous studies, we are the first to estimate the economic costs affected by the nonpharmaceutical interventions through an innovative model via observable CO_2 emissions. Though the validation of this model conducted in this article is based on historical datasets, our model can also run in a real-time or near real-time mode. Specifically, we quantify a model capable of connecting the daily changing rate of confirmed COVID-19 cases to the daily variation of CO_2 emissions in city-level prefectures. Due to the containment of CO_2 emissions, economic activities are inevitably constrained, and thus, the gross domestic product (GDP) loss can be measured based on the CO_2 emissions. Therefore, we also build the relations between the CO_2 emissions reduction and GDP loss in China.
3) We innovatively process the mobile-phone geolocation data on a daily basis to quantify the sequential transmission risk of any prefectures outside the epicenter. Then, a data model, namely, the risk source model, is proposed from real-time information on population movements and the epidemic to identify the regions with high local transmission risks. Risk index values, higher than the upper bound of a certain confidence interval (CI) (e.g., 90% or 95%), can be used as warning information and a practical measure to assist the decision on whether and when more stringent measures should be adopted.
4) Finally, we integrate the high-resolution artificial society with the data-based models to evaluate and tailor interventions through large-scale computational experiments. Validations of our approach are carried out in four artificial societies: Wenzhou, Guangzhou, Beijing, and Wuhan. Especially, we explore when and to what extent the lockdown measures are necessary for a prefecture. Our findings reveal that the local transmission of a city can be almost contained if lockdowns are adopted immediately when the risk index is higher than the upper bound of a certain CI. Moreover, the

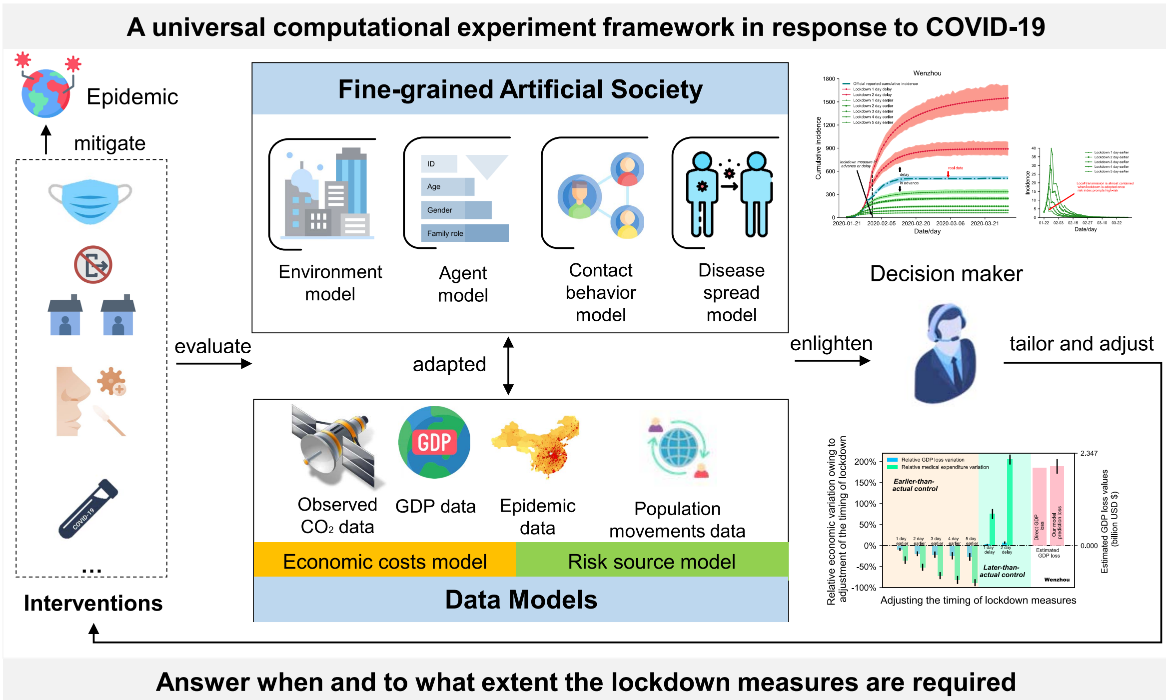

Fig. 1. Workflow of the proposed universal computational experiment approach.

necessity of advancing the timing of lockdown measures both in limiting the spread of COVID-19 and in economic benefits at the early stage of the epidemic is also elucidated.

II. Methodology

This article involves many models from various sources. Here, we only introduce the main items involved in the results. More details about the construction of artificial society and how we carry out the computational experiments can be referred to in our previous study [21], [22].

A. Workflow of the Proposed Approach

As shown in Fig. 1, we describe the process of how to leverage our universal computational experiment approach to evaluate and tailor interventions. First, a high-resolution agent-based artificial society is established, including environmental models, agent models, contact models, and disease models. The details of the construction of the artificial society can be referred to these studies [22]–[25]. Then, by sorting out various nonpharmaceutical interventions and quantifying the impact of different measures, an eight-tuple strategy model is proposed [22]; subsequently, the economic cost model of an intervention strategy is proposed based on observed CO_2 emissions data, epidemic data, and GDP data. Moreover, a risk source model is built based on population movement data and epidemic data. Finally, by integrating data models with the artificial society, large-scale computational experiments can be carried out to study the effects of various strategies, to design suitable interventions, to realize tradeoffs between economic development and epidemic control, and to decide whether the lockdowns are necessary. The results and implications from experiments can assist decision-makers to tailor existing intervention strategies.

B. Intervention Strategy Model

We propose an eight-tuple strategy model, denoted as (1), to parameterize the governmental response to contain the pandemic. The model mainly includes social distancing, personal protection, throat swab testing capability, quarantine of contacted persons and case isolation, area blockade, random testing, suspected monitoring, and time to execute the measures. A detailed description of each parameter in the model is provided as follows:

$$I^t = \langle NC^t, PI^t, CT^t, QC^t, AB^t, RT^t, ST^t, \Delta t \rangle. \tag{1}$$

NC^t: The average number of contacted persons in a day. This parameter is often used to indicate the intensity of social distancing. In this study, we used the method of Box–Muller [26] to generate NC^t, as formulated in (2), in which $NC^{t'}$ is the mean value, σ is the standard deviation, and r_1 and r_2 are uniformly distributed random numbers between [0, 1]

$$NC^t = NC^{t'} + \sigma(-2\ln r_1)^{1/2}\cos(2\pi r_2). \tag{2}$$

PI^t: The probability of being infected outside. We use this parameter to reflect different intensities of environmental decontamination and personal protection. The parameter is determined at 0.05249 with a 95% CI [0.05068, 0.05429] when no mitigation measures are taken [27].

CT^t: Capability of throat swab testing. According to the data disclosed by different countries, it can be assumed

that the daily testing capacity increased linearly during the transmission period of COVID-19, formulated as $CT^t = CT^{T_e} \times \Delta t/T_e$. T_e is the duration from the first day applying polymerase chain reaction (PCR) diagnostic reagents to the end of observation, t is the time point to execute the current measure, and CT^{t_e} denotes the test capability at the end of observation [28].

QC^t: Conduct quarantine if contacted with the diagnosed patients. It determines the state of a person who contacts with a diagnosed case would be quarantined.

AB^t: Block the traffic to other districts, and restrict access to communities. This parameter quantifies the measure of area blockade and determines whether the spread of COVID-19 across other districts is invalid.

RT^t: Random test for the citizens. The measure conducts random sampling tests for prefectures with severe epidemics.

ST^t: Nucleic Acid Test for suspected patients. This parameter is determined by governmental policy and medical resources.

Δt: Time duration from the occurrence of the first patient (t_0) to the implementation day of the current measure ($\Delta t = t - t_0$).

As time goes on, the intervention strategies of a prefecture would change according to the situation of COVID-19. Assume that the strategy varies at time t_0, t_1, t_2, and so on, and the intervention strategy of a prefecture i for a long period can be denoted as

$$I_i = \langle I_i^{t_0}, I_i^{t_1}, I_i^{t_2}, \ldots, I_i^{t_n}, \ldots \rangle. \tag{3}$$

C. Economic Costs' Model

The economic costs of an intervention strategy include medical expenditure and GDP loss. Here we build the relationship of the epidemic to daily CO_2 emissions; as for models of medical expenditure and the relationship of CO_2 emissions to GDP can be referred to in our previous study [22].

First, we detrend the estimated CO_2 emissions by removing a temporal trend from 2016 to 2019. This action can better show the impact of COVID-19 on CO_2 emissions in 2020, as shown in the following equation:

$$E_{hit_y}^{\text{detrended}} = E_{hit_y}^{\text{original}} + \left(2020 - t_y\right) \cdot \xi_m \tag{4}$$

where h is a month, i is a prefecture, t_y is a year, ξ_m is the linear regression slope of $E_{hit_y}^{\text{original}}$ against year t_y, and $E_{hit_y}^{\text{original}}$ is the daily average in month h, in the unit of (gram carbon/m^2/day).

Then, the daily change in CO_2 emissions is estimated from the starting day of the epidemic to a given end day based on the concentration confinement factor (CCF) computed through NO_2 column concentrations [18]. It is assumed that COVID-19 did not contribute considerably to changes in NO_2 column concentration in December between 2015–2018 and 2019, which serves as a reference change in the absence of COVID-19. Therefore, the estimated changes in daily CO_2 emissions with COVID-19 relative to a reference without COVID-19 are formulated as

$$\Delta E_{ji} = E_{ji} - E_{0ji} = E_{0ji} \cdot \left(\text{CCF}_{ji} - 1\right) \tag{5}$$

$$\Delta E_{ji} = \frac{\overline{E_{hi,2016-2019}}}{n_h} \cdot \frac{\overline{E_{0i,2019}}}{\overline{E_{0i,2015-2018}}} \cdot \left(\text{CCF}_{ji} - 1\right) \tag{6}$$

where j is a day; E_{ji} and E_{0ji} are the daily CO_2 emissions with and without COVID-19, respectively; $\overline{E_{hi,2016-2019}}/n_h$ is the daily detrended CO_2 emissions as an average for 2016–2019; $\overline{E_{0i,2019}}$ and $\overline{E_{0i,2015-2018}}$ are the detrended CO_2 emission in December 2019 and the detrended average for December 2015–2018, respectively; CCF_{ji} denotes the concentration change on a given day relative to an average of the same days during 2016–2019; and we took advantage of the results about CCF given in [18].

Subsequently, we use two indicators $W_{j,g}^i$ and $Z_{j,g}^i$ to denote the change in daily confirmed cases and daily CO_2 emissions reduction and develop a regression model between the two indicators for a prefecture i as

$$W_{j,g}^i = a_i \cdot Z_{j,g}^i + b_i \tag{7}$$

where a_i is the slope and b_i is the intercept of the regression, respectively. We compare the fitting results between several pairs of the two indicators and, finally, determine $W_{j,4}^i$ and $Z_{j,4}^i$ according to R^2 and p-value (see [22])

$$W_{j,4}^i = \begin{cases} 0, & N_{ji} \text{ and } N_{(j-1)i} = 0 \\ \ln\left(\dfrac{\left(N_{ji}+1\right)}{j \cdot \left(N_{(j-1)i}+1\right)}\right), & N_{ji} \text{ or } N_{(j-1)i} \neq 0 \end{cases} \tag{8}$$

$$Z_{j,4}^i = \frac{\Delta \text{TER}_{ji}}{\text{TER}_{0i}} = \frac{\sum_{d=1}^{j} \Delta E_{di}}{\sum_{d=1}^{t_{\text{end}}} E_{0di}} \tag{9}$$

where N_{ji} is the number of daily new confirmed cases in day j at prefecture i; d is a day; and t_{end} is the given last day. Therefore, ΔTER_{ji} denotes total CO_2 emissions reduction due to COVID-19, while TER_{0i} is the total CO_2 emissions without COVID-19.

D. Risk Source Model

We use the following multiplicative exponential model to model the effect of outflows on infections on a given day:

$$cy_i = c \cdot \sum_{f=1}^{m} e^{\beta_f \cdot x_{fi}} e^{\sum_{k=1}^{n} \lambda_k \cdot P_{ik}} \tag{10}$$

where cy_i is the number of the cumulative (or daily) incidence in prefecture i; x_{fi} denotes the predictor variable affecting the prediction of cy_i; specifically, x_{1i} is the cumulative population outflow from Wuhan to prefecture i from January 1 to 24, 2020; x_{2i} and x_{3i} represent the GDP and the population of a prefecture i, respectively; and m is the number of variables included. c and β_f are parameters to estimate. In the above models, λ_k is the fixed effect for province k; n is the number of prefectures considered in the analysis; and P_{ik} is a dummy for prefecture i and $P_{ik} = 1$ if $i \in k$ (prefecture i belongs to province k); otherwise, $P_{ik} = 0$.

The parameters of the above model are estimated by applying a nonlinear least-squares method (i.e., the Levenberg–Marquardt algorithm [29]) with cy_i as the dependent variable and x_{fi} as the predictor variables. Using the predicted incidence data in model (10), we are able to compute a daily risk score for prefectures considering the relative difference between the number of predicted and reported incidence on any given date. Prefectures with a higher-than-expected score on the risk index are noteworthy since they are undergoing severe local community transmission with a high probability.

We extend the model (10) into a dynamic one to explore changes in distribution and growth of the epidemic across all prefectures over time. To combine the previous daily analysis with time and fixed effects to control for provincial differences, we leverage a Cox proportional hazards framework to integrate the risk source model (10) with a growth function $\lambda_0(t)$, which allows the epidemics typically follow

$$\lambda(t|x_i) = \lambda_0(t) \cdot \sum_{f=1}^{m} e^{\beta_f \cdot x_{fi}} e^{\sum_{k=1}^{n} \lambda_k \cdot P_{ik}} \tag{11}$$

where $\lambda(t|x_i)$ is the hazard function describing the number of cumulative incidence at time t given a population outflow from the epicenter to any prefecture i; $\lambda_0(t)$ is the underlying baseline hazard function with $t = 1$ starting from January 24, 2020; $x_i = \{x_{1i}, x_{2i}, \ldots, x_{mi}\}$ denotes the realized values of the covariates for prefecture i; and the other notations are the same as for model (10). In particular, model (11) captures the effect of risk source outflow from Wuhan in a spatiotemporal manner.

We consider the three most popular sigmoidal functions (i.e., the logistic model, the Richards model, and the Gompertz function) [30]–[32] for $\lambda_0(t)$ in the hazard model (11) and use the same method as before to estimate the unknown parameters. With this estimation and reported incidence data, a total transmission risk index can be built.

III. Experiments

In this section, we first introduce the data sources and then conduct calibration, sensitivity, and validation experiments of our models. Subsequently, the results of two data models are given. Finally, large-scale computational experiments on counterfactual scenarios are conducted to illustrate how to adjust interventions to achieve better results in economic development and epidemic control with the actual scenario as a reference.

A. Data Sources

Here, we only briefly introduce the main data used and its sources. With regard to the observable CO_2 emissions data, it refers to two different data, and one is daily CO_2 emissions' concentration data, while the other one is the estimated amount of monthly CO_2 emissions data. The CO_2 emissions' concentration data were compiled from the ODIAC Fossil Fuel Emission dataset (https://db.cger.nies.go.jp/dataset/ODIAC/). The method and data for estimation of monthly CO_2 emissions during 2016–2020 can be referred to in [18]. Moreover, the quarterly GDP data from 2016 to 2020 in different cities of China were compiled from the statistics of the National Bureau of Statistics of China. As for the epidemic data, we compiled the COVID-19 global pandemic trend on each day released by the COVID-19 Global Pandemic Real-Time Report (https://ncov.dxy.cn/ncovh5/view/pneumonia). Besides, we also used a complete dataset, describing the population outbound flow from Wuhan during the outbreak of COVID-19 in 2020 (https://spj.sciencemag.org/journals/hds/2021/9796431/).

B. Calibration, Sensitivity, and Validation of the Constructed Artificial Society

We first calibrate the input parameters to obtain key characteristics in line with epidemiological data on COVID-19. The reliability of outputs generated by our models is ensured by comparing epidemiological indicators [i.e., reproductive number (R_0), generation period (T_{gen}), and growth rate of the cumulative case ($\dot{C}$)] to the mean of output variables. The output results are acquired from stochastic Monte Carlo simulations during no-mitigation periods, with CIs estimated by a bias-corrected accelerated nonparametric bootstrapping approach [33]. In accordance with available data announced by authoritative bodies and previous studies [34]–[36], the output variables include $R_0 = 3.628$, 95% CI [3.577, 3.684] with number of simulations at 12 000; $T_{\text{gen}} = 9.102$, 95% CI [8.942, 9.269] with number of simulations at 12 000; and $\dot{C}) = 0.166$, 95% CI [0.164, 0.168] with number of simulations at 500 in the Wenzhou artificial society. The mean of output variables is considered reasonable, and the relatively narrow CIs reflect the intrinsic stochasticity of the simulations.

Then, we apply a global sensitivity analysis [37] to testify to the robustness of our constructed models and their outcomes. This analysis is used to obtain elementary effects by measuring the response of a targeting output variable to the change in an input parameter. In this study, we select these input parameters: ix_1: the probability of a person transforming from the susceptible state to the infected state; ix_2: the probability of a person transforming from the infected state to the sick state; ix_3: the probability of a person transforming from the sick state to the recovered state; ix_4: the incubation period; and ix_5: the period from the infected state to the recovered state. We compute the mean μ_i^* of the absolute response and the standard deviation σ_i of each input parameter. Smaller values of μ_i^* and σ_i indicate the lower sensitivity of the output parameters. As seen in Table I, we know that R_0 and T_{gen} are most sensitive to changes in the incubation period (T_E) but also stay within the expected ranges (e.g., R_0 varies between 1.921 and 4.054, and T_{gen} varies between 8.283 and 11.902). The daily growth rate of cumulative incidence $\dot{C}$ shows small global sensitivity to all input parameters. It is concluded that the model is robust to changes in the input parameters.

Subsequently, the validation against the actual epidemic timeline in Wenzhou city is performed. Through collecting pandemic data and intervention strategies from January 1 to March 31, 2020, we quantitatively model the strategies, parameterize the strategy model according to the actual timeline, and simulate the spread of COVID-19 in Wenzhou. The timeline of interventions in Wenzhou is drawn in Fig. 2, and the

TABLE I

INPUT PARAMETERS ix_i AND OUTPUT VARIABLES y_j: GLOBAL SENSITIVITY ANALYSIS WITH THE EFFECT $|EE_i|$

Parameters	***Range***	$R_0(y_1)$		$T_{\text{gen}}(y_2)$		$\dot{C}(y_3)$	
		$\sigma_{i,1}$	$\mu^*_{i,1}$	$\sigma_{i,2}$	$\mu^*_{i,2}$	$\sigma_{i,3}$	$\mu^*_{i,3}$
PI^t (ix_1)	[0.05068-0.05429]	0.703	0.545	1.407	0.992	0.008	0.008
α (ix_2)	[0.50-0.95]	0.418	0.314	0.940	0.728	0.008	0.007
β (ix_3)	[0.950-0.991]	0.866	0.672	1.439	1.129	0.012	0.010
T_E (ix_4)	[3.0-7.0]	0.964	0.703	1.764	1.381	0.011	0.009
T_I (ix_5)	[6.0-15.0]	0.708	0.528	1.760	1.198	0.012	0.014

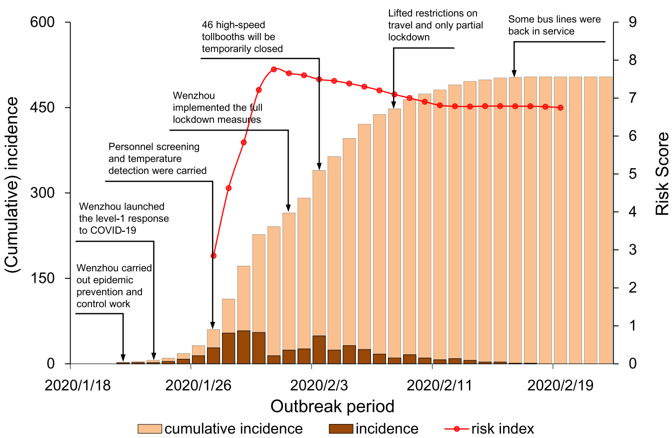

Fig. 2. Actual timelines of epidemic spread and mitigation measures in Wenzhou along with the risk score.

TABLE II

QUANTITATIVE RESULTS OF INTERVENTION STRATEGY IMPLEMENTED IN WENZHOU

NC^t	PI^t	CT^t	QC^t	AB^t	RT^t	ST^t	Δt	**Real time**
15.2	0.0524	0	0	0	0	0	0	20.01.20
14.2	0.052	500	1	0	0	1	3	20.01.23
4.9	0.0272	2000	1	1	0	1	12	20.02.01
3.05	0.025	2800	1	1	0	1	14	20.02.03
5.05	0.0005	3500	1	0	0	1	19	20.02.08
8.99	0.0005	6500	1	0	0	1	21	20.02.10

values of input parameters are determined in Table II. As we can see, the number of simulated (cumulative) incidences is very close to the number of reported (cumulative) incidences, as shown in Fig. 3(a). From the fitting results [see in Fig. 3(b)], it is found that the simulation in Wenzhou obtains a satisfied performance with a high R^2 and low p-value. The results reveal the validity of our constructed models.

C. Correlation Analysis Between the Daily Confirmed COVID-19 Cases/GDP and CO_2 Emissions in China

Fig. 4 shows the COVID-related variations in monthly averaged estimates of CO_2 emissions between January and May 2020 compared to 2019. In the aggregate, China's CO_2 emissions were about 7.61% lower in January and February, 5.06% lower in March, 2.02% higher in April, and 5.99% higher in May 2020 relative to the same months in 2019. The decline or the rebound in monthly averaged CO_2 emissions time series was synchronous with domestic strict lockdown measures, which were relaxed from March and April.

Due to the disruption in economic activities caused by COVID-19 and strict lockdown measures, we also observe a sharp decline in GDP in the first quarter of China. In the aggregate, the relative differences between 2020 and 2019 were -3.25% in the first quarter but reached $+5.31\%$ (greater in 2020 than 2019) in the second quarter as economic activities fully resumed in China from April.

The results suggest that the reduced economic activities (GDP loss) and CO_2 emissions are greatly associated with the lockdown measures. Therefore, we take CO_2 emissions as a bridge and model the impact of intervention strategies on economic costs C_I from two main aspects, namely, the GDP loss and medical expenditure. As shown in the following equation, Me_I represents the medical expenditure, G_I represents the GDP loss, and I indicates different strategies:

$$C_I = Me_I + G_I. \tag{12}$$

Based on the above observations, we perform an analysis of the correlation between newly increased COVID-19 cases (incidence) and the daily CO_2 emissions reduction. The fitting results indicate that the CO_2 emission indicator $Z_{j,4}$ and the daily confirmed cases indicator $W_{j,4}$ are fit with the best performance ($R^2 = 0.96$ and $p < 0.001$) by a linear regression model, for example, formulated as $W_{j,4} = -12.35 \cdot Z_{j,4} - 0.23$ for Wenzhou. We also verify this point in other cities. Detailed statistics of the correlation analysis are shown in Fig. 5.

Furthermore, we compute the GDP loss based on the reduction of CO_2 emissions in target cities. The data used in the model were chosen from 2016 to 2019 since China enacts a "five-year plan" to set out its economic development goals every five years, during which the growth rate of GDP is relatively stable, and the CO_2 emissions are regularly increasing within the five years [38]. With the above models, we are able to quantify the impact of different intervention strategies on GDP loss in a city. The validity of the constructed model was testified through the comparison between the GDP loss obtained by the abovementioned models and the GDP loss computed by the trend forecast model. The relative difference between the two GDP losses is about 2.04% in Wenzhou. Moreover, we also estimate the medical expenditure for cured cases and mortality costs for fatal cases during the COVID-19 pandemic (related models see in our previous study [22]). With this result, we are capable of estimating the economic costs of any implemented intervention strategies.

D. Outflow From Epicenter Drives the Distribution of the Confirmed COVID-19 Cases in China

We link the aggregated outbound flows from Wuhan during the first month of the outbreak to COVID-19 infection counts at other prefectures. As shown in Fig. 6(a), the distribution of the outflow and cumulative cases is depicted with geographical information. As the epidemic evolved, stringent quarantine measures were imposed in Wuhan and its neighboring prefectures (first in Wuhan at 10:00 on January 23, 2020). Therefore, we observe a dramatic drop in the population outflow from Wuhan to other prefectures, manifested in a reduction of 93.89% population outflow (main provincial cities outside Hubei province) on January 24, 2020, compared with January 23, 2020 [see Fig. 6(b)]. Later on, population outflow from

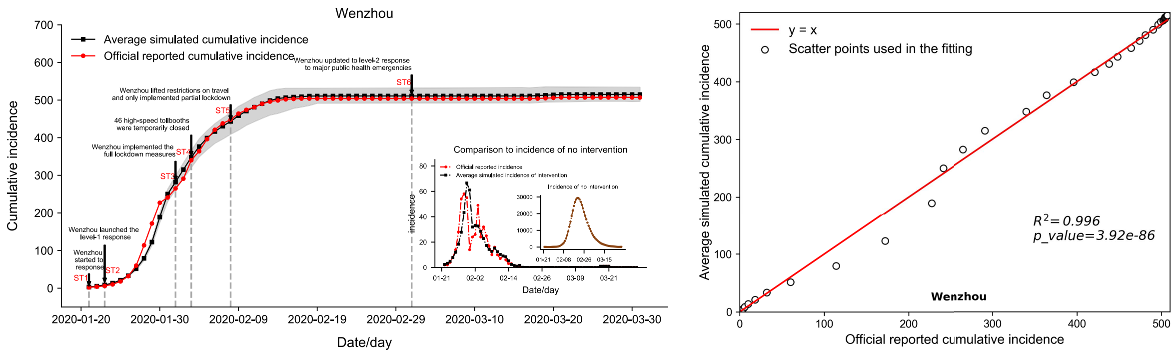

(a) (b)

Fig. 3. Validation against actual epidemic timeline in Wenzhou. (a) Epidemic (COVID-19) spreading in Wenzhou. (b) Scatter plot of reported cases versus simulated cumulative cases in Wenzhou.

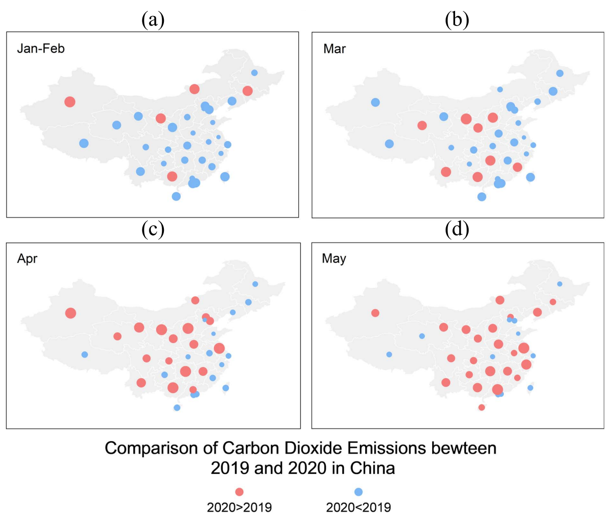

Fig. 4. Spatial distribution of changes in activity-based CO_2 emissions. Since the activity data are compiled as a total for January and February, the data for January and February are considered together. (a) Emission comparison in January-February. (b) Emission comparison in March. (c) Emission comparison in April. (d) Emission comparison in May.

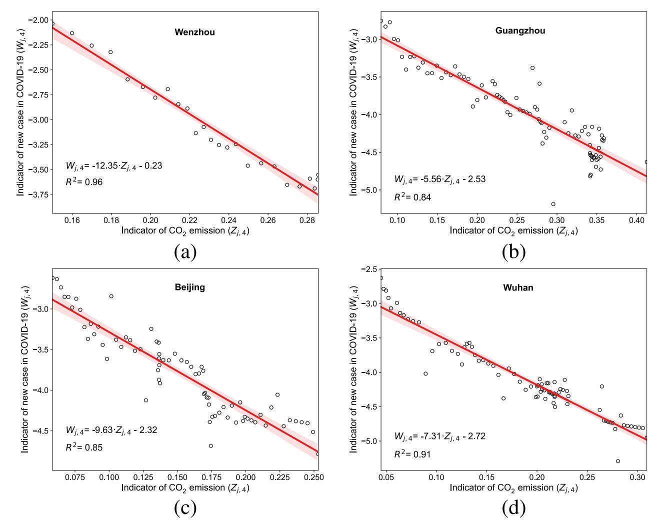

Fig. 5. Correlation between the indicator of daily confirmed COVID-19 cases and the indicator of CO_2 emissions reduction. (a) Wenzhou. (b) Guangzhou. (c) Beijing. (d) Wuhan.

Wuhan almost completely stopped, evidenced by the fact that daily outflow (average) thereafter was just about 1087 people to all prefectures outside of Hubei.

We then perform a time-dependent correlation analysis between the total population outflow from January 1, 2020, to January 22, 2020, and the confirmed number of infections in the main provincial cities of China. Consistent with previous findings [20], [39], results indicate a strong correlation between the two variables, and the strength increases over time [see Fig. 6(d) and (e)]. It is also observed that a similar robust pattern exists in the correlation when different time windows of population outflow or cumulative incidence are used. As for cumulative incidence, the coefficients are 0.62 (0.57–0.63, $p < 0.001$) on January 25 and the correlations peak on February 3, 2020, indicating that the transmission pattern of COVID-19 gradually converges to the distribution of the population outflow from Wuhan to other cities in China.

Leveraging data about population outflow from the epicenter, a risk source model [39] is developed to signal the risk levels of COVID-19 community transmission for the prefectures outside the epicenter

$$\Psi_i = \sum_{t=1}^{T} \left[\lambda(t|i) - \hat{\lambda}(t|x_i)\right] \tag{13}$$

where $\lambda(t|i)$ is the cumulative number of confirmed cases at time t for prefecture i, $\hat{\lambda}(t|x_i)$ is the estimated cumulative number of cases by our hazard models at time t for prefecture i, and T is the total time period (days) considered. We derive the final transmission risk index $\overline{\Psi_i}$ by leveraging the integral of the differences over time (normalize the measure Ψ_i by subtracting the mean and dividing by the standard deviation) and use this index to identify the local transmission risk level for different prefectures. Prefectures above a setting CI (e.g., 90% or 95%) of the index are likely experiencing more local transmissions than imported cases. As shown in Fig. 6(c), the dynamic shifts in the risk index score for selected cities are depicted, which enables us to judge whether a city performs well in containing the transmission of COVID-19 over time.

When the value of risk index $\overline{\Psi_i}$ is larger than 1.645, 1.960, or 2.576, the corresponding prefectures have a statistically significant transmission risk at the 90%, 95%, or 99% CI, respectively. We statistically count the top-ten prefectures on the

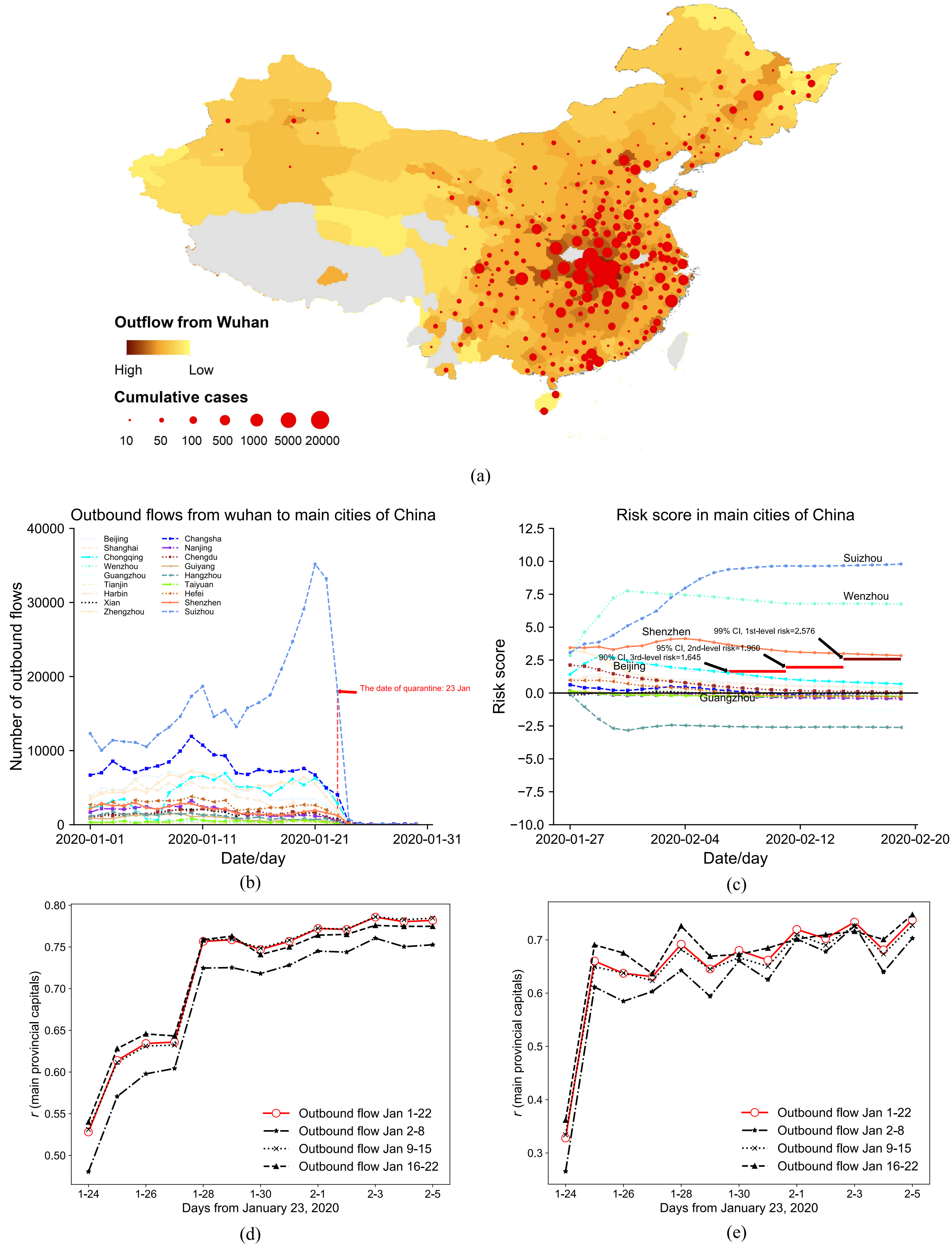

Fig. 6. Geographic distribution of population outflow, as well as (cumulative) incidence and strength of correlation between them by the length of observation days. The white area indicates grid points with missing data. (a) Geographical distribution of aggregate population outflow from Wuhan until January 23, 2020, and the cumulative incidence in other Chinese prefectures. (b) Aggregate outbound flows from Wuhan to the main provincial cities of China over time. (c) Risk scores over time in main provincial cities of China. (d) Strength of correlation between outbound flows from Wuhan and the number of confirmed cumulative cases by the length of observation days. (e) Strength of correlation between outbound flows from Wuhan and the number of confirmed daily cases by the length of observation days.

transmission risk index from January 27, 2020, to February 19, 2020, and discover that Suizhou, Wenzhou, Xiaogan, and Shenzhen have a highly significant transmission risk score above 99% CI. As the first prefectures to be quarantined outside of Hubei, Wenzhou adopted lockdown measures since the start of February 1, 2020. The scores in the risk index indicate that Wenzhou (risk index = 7.65) showed poor performance in local transmission containment before February 1, 2020.

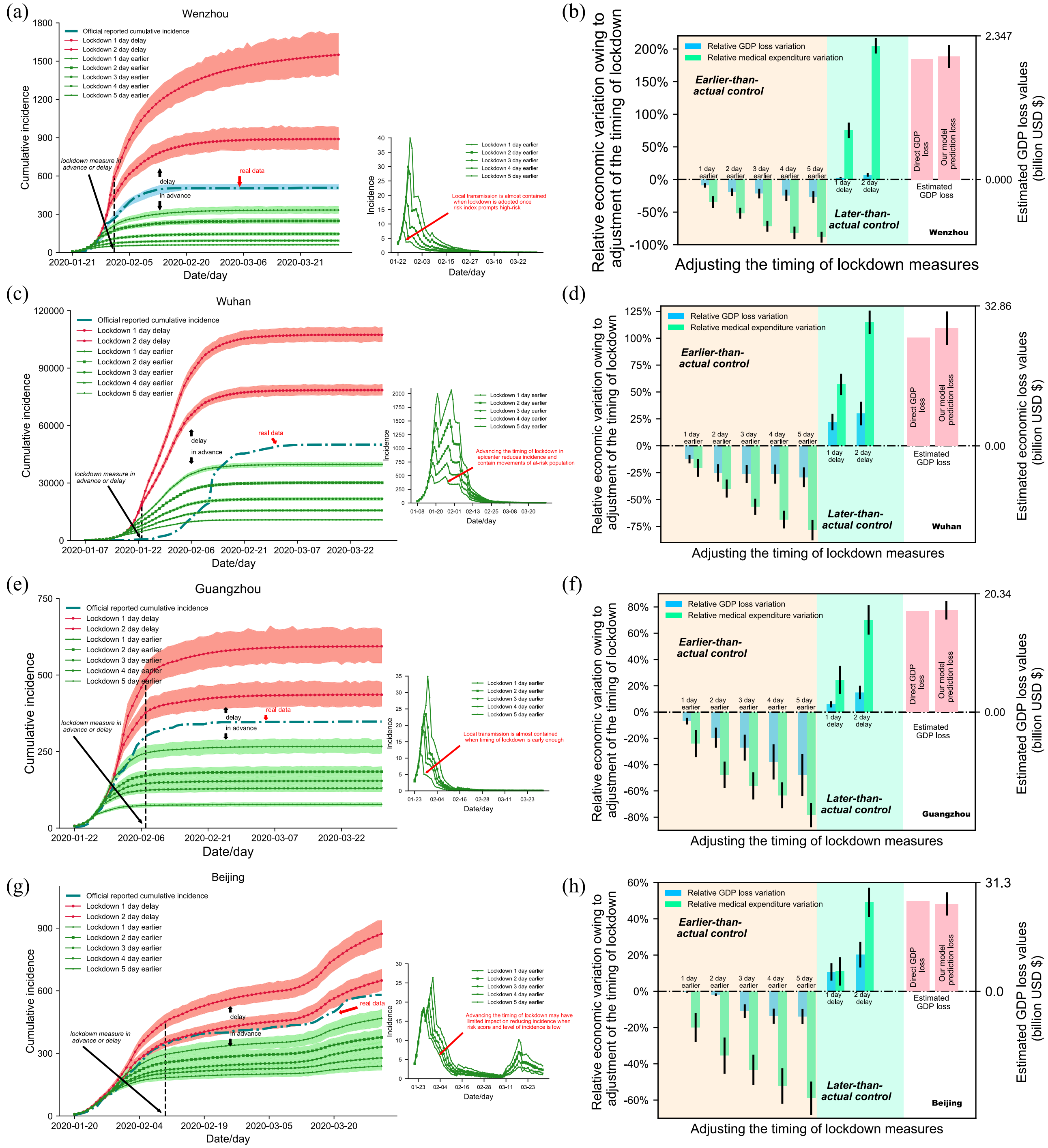

Fig. 7. Sensitivity of the (cumulative) incidence and economic costs to the starting day of lockdown in Wenzhou, Wuhan, Guangzhou, and Beijing. (a), (c), (e), and (g), the simulated (mean and 95% CI) cumulative cases with the 95% CIs denoting the uncertainty for Wenzhou, Wuhan, Guangzhou, and Beijing are presented. The red dashed line represents the reported cumulative cases and the target strategy denotes the lockdown measures. The results of anticipating or delaying the target strategy are differentiated by the red dashed line. (b), (d), (f), and (h), the variations of economic costs for Wenzhou, Wuhan, Guangzhou, and Beijing according to the adjustments of the timing of lockdown measures are presented. Our predicted GDP losses are close to the direct GDP losses and the timing of lockdown measures earlier than actual control is beneficial to the reduction of both GDP loss and medical expenditure. The error lines denote the 95% CIs.

It reveals that the Wenzhou government had lagged behind in its lockdown strategy at that time. Therefore, when the real-time risk index prompts risks, computational experiments should be carried out in time on evaluating interventions so that the intervention strategy and its intensity can be better adjusted.

E. In-Advance Lockdowns Can Facilitate Pandemic Control and Economic Development

Inspired by the risk score, we investigate the counterfactual scenarios aimed at estimating the impact of anticipating or delaying lockdown measures on the transmission of COVID-19 in different cities. Taking Wenzhou as an example, we simulate the epidemic when the starting day of lockdown measures was enforced one to five days earlier or one to two days later relative to the actual scenario. From Fig. 7(a), we observe that it would lead on average to a 74.95% (95% CI: [60.16%–95.27%]) more intense cumulative incidence peak if the start of lockdowns was executed one day later compared to that in the actual scenario. The increase in cumulative incidences would be more pronounced as the lockdowns are delayed, indicating that the number of cumulative incidences is sensitive to the lockdown measures at the early stage. In contrast, an earlier lockdown incurs a less intense cumulative incidence peak, evidenced by the number of peak cases reduced from around 34.71% to 88.16% on average if the lockdowns were enforced one to five days earlier. If the lockdown measures were implemented once the risk index prompts high local transmission risk on January 27, 2020, the number of confirmed cases in Wenzhou would be limited to around 58.76 on average (95% CI: [54.98–62.66]). Similar to the simulation conducted in Wenzhou city, we also simulated the transmission of COVID-19 in Wuhan, Guangzhou, and Beijing when the starting day of lockdown measures had been enforced one to five days earlier or one to two days later relative to the actual scenario, as shown in Fig. 7. On the whole, we witnessed a similar trend in the epidemic spread when adjusting the timing of the lockdown measures. However, if the lockdown measures or intervention strategies were not adopted, the figure of cumulative incidence peak would increase to more than 1000-fold compared to that in the actual scenario. In terms of Wuhan, more than three-quarters of the population eventually became infected when no intervention strategies were implemented; more than half of the population became infected in other cities. It implies that the local transmission can almost be contained if stringent strategies are adopted at the initial stage of the epidemic, which is consistent with findings in previous studies [40], [41].

Based on the official reported data of cumulative incidences, the GDP loss and medical expenditure on containing COVID-19 in Wenzhou are estimated at 2.01 and 0.069 (unit: billion dollar), respectively. In terms of the changes in economic costs incurred by changing the starting day of lockdown measures, we use the GDP loss obtained by implementing lockdowns on February 1, 2020, as a reference and witness a gradually decreasing trend in GDP loss if the lockdown was enforced one to five days earlier. The reduction in GDP loss is from around 9.15% to 27.09%, indicating that the GDP loss can be greatly reduced by implementing in advance lockdown measure, while other intervention strategies remain unchanged, as shown in Fig. 7(b). This variation in Guangzhou is more distinct, the figures of which range from 6.92% to 47.94%, as shown in Fig. 7(f). We then compute medical expenditure for cured cases and the mortality cost for fatal cases in the actual situation and counterfactual scenarios. The medical costs range from 0.008 (billion dollar) to 0.211 (billion dollar) on average when the time of lockdown changes from January 27, 2020, to February 3, 2020, for Wenzhou. These results confirm not only epidemic control but also the economic benefits from the advanced timing of lockdown measures by leveraging the information of the risk index.

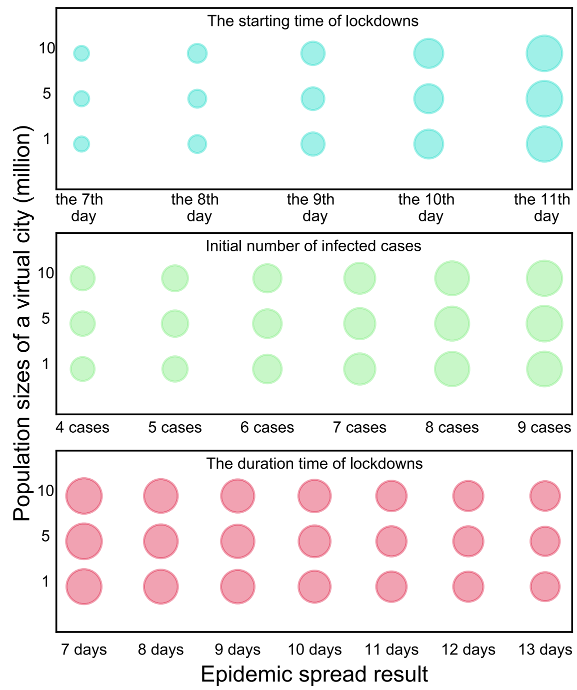

Fig. 8. Sensitivity of the (cumulative) incidence to population sizes of a city w.r.t. initial number of infected cases (reflecting the initial transmission threat), the starting time of lockdowns, and the duration time of lockdowns.

We finally investigate the effects of interventions (the base strategy is set as the Wenzhou strategy) in an artificial city of various population sizes (i.e., one million, five million, and ten million people). Specifically, the sensitivity of the (cumulative) incidence to population sizes of a city w.r.t. the initial number of infected cases (reflecting the initial transmission threat), the starting time of lockdowns, and the duration time of lockdowns are tested, as shown in Fig. 8 (the size of a circle denotes the average confirmed infected cases in the simulation). As the increment of initial transmission risk, the mean infected cases continue to increase, changing from 120.29 (95% CI [108.19, 138.06]) to 256.98 (95% CI [239.57, 275.02]) in the one million artificial society. It indicates that, with an early lockdown available in the intervention, the mass local transmission would occur when the initial transmission threat becomes high. The trend is also true for an artificial society of five million and ten million people. In addition, the sensitivity results of the cumulative incidence to the duration time of lockdowns reveal that lockdowns lasting for 7–14 days in prefectures would be effective in controlling the spread of the epidemic. To effectively contain the outbreak, the duration of lockdowns should be prolonged when the initial transmission threat becomes greater. Under the same experimental settings, the experimental results of the artificial city with different population sizes are close, indicating that the city governors should be alert to start the lockdown measures as early as possible no matter the population size of their cities when the initial transmission threat is high.

Detailed results can be found in Tables S1 and S2 in the Supplementary Material.

IV. Discussion

In this study, we first simulated the spread of COVID-19 in Wenzhou. The artificial society of Wenzhou was calibrated to known pandemic dynamics and considered social context-dependent activities, social and household relationships, and other relevant epidemiological parameters. The robustness of our model was also verified through sensitivity analysis. From the comparison between the simulated results with the official reported information, it is interesting to note that the peak of simulated incidence is in line with the peak of actual incidence, and the time of which is earlier than the peak time of incidence occurred in the situation with no interventions.

We then analyzed the relationships between epidemic control and economic costs by using the CO_2 emissions as a bridge. It is confirmed that the daily rate of incidence is lowered by containing more economic activities, and as a result of which, more CO_2 emissions are reduced. From the comparison between medical expenditure under the actual scenario and no intervention situation, it can be concluded that avoiding the costs in the short term incurred by the intervention policies creates a substantial loss tenfold larger in medical expenditure and would face more GDP loss in the long term due to the occurrence of recurrent epidemic outbreaks. Also, it is interesting to note that, if the intervention strategies were delayed for several days, enhancement of the strength of control required to limit cumulative incidence cases at the same level within the actual scenario would cause greater damage to the economy.

We also analyzed the correlations between aggregate outflows from the epicenter and cumulative incidence in other prefectures. Based on that, we established a dynamic risk source model to quantify the burden of community transmission. The score of the risk index is able to anticipate the subsequent location, intensity, and timing of local outbreaks outside the epicenter. Notably, prefectures (e.g., Suizhou and Wenzhou) identified with high scores of risk index up to February 19, 2020, had experienced severe local outbreaks. This model can accommodate multiple risk sources for countries with multiple disease epicenters. It can also be extended to a live fashion if real-time mobility data are available.

We finally leveraged the data-based models in the dedicatedly designed counterfactual simulated scenarios. Results reveal that anticipating the timing of lockdown measures is beneficial to pandemic containment and economic losses. Notably, if the lockdown measures are adopted in the prefectures once the risk source model prompts a high risk of community transmission, the local transmission can be almost completely contained, as observed in Wenzhou if the lockdown were advanced five days earlier. It indicates that, in the early stage of the outbreak, if the lockdown measures are implemented as early as possible, the epidemic can be controlled in a short time, and the national economy can be minimally affected.

Overall, our study offers a fresh new prospect of combining data-analytic and high-resolution simulation techniques to contain COVID-19. Our approach is generalizable in many aspects: 1) the high-resolution agent-based artificial society modeling approach is generalizable to any prefectures (e.g., city level, provincial level, or national level) with available population and geoenvironmental data; 2) the correlations between daily rate of incidence and CO_2 emission reduction can be generalized to datasets at provincial, national, and global levels; and 3) the method aggregating population flows can be generalized to any datasets that reflect population movements, such as train-ticketing or air transportation.

V. Conclusion

Understanding the necessity and economic benefits of lockdown measures is important for policy-making. To this end, we construct a high-resolution agent-based artificial society, which was adapted to real-time data and integrated with data-based models. Through observable CO_2 emissions, we are able to estimate the economic costs of intervention strategies based on a model, which connects incidence data and the variations of GDP. Moreover, a risk source model is built based on the relations between the COVID-19 cases and population outflows from the epicenter for estimating the local transmission risk. Observed in sensitivity analysis and validation experiments, our models show high accuracy in predicting both infection cases and economic costs. Through large-scale computational experiments, our research findings provide many implications for policy-making, for instance, in-advance lockdown measures should be adopted when the local transmission risk is higher than the upper bound of a certain CI. The combined data-and-simulation approach is important for decision-makers to understand the possible spread of the epidemic, as well as whether and when lockdown measures are required.

While the proposed approach has provided insightful implications in decision-making, we can still explore the following aspects further. Reporting errors and delays are likely to have occurred in officially reported case data; though our model estimate is relatively accurate, it can also be improved by enhancing the capability of detecting and calibrating such delays. The models of economic decline and pandemic control in this study are based on the CO_2 emissions data in a fixed period (e.g., five consecutive years) in China. To make the prediction more generalizable, future work can use deep learning approaches to predict GDP based on CO_2 emissions. Moreover, we acknowledge that the models and evaluations of this work were only verified on historical datasets. In the future, we could consider dynamic calibration and assimilation of real-time data in the ongoing epidemic.

References

[1] T. Velavan and C. Meyer, "The COVID-19 epidemic," *Tropical Med. Int. Health*, vol. 25, no. 3, p. 278, 2020.

[2] L. Li *et al.*, "Characterizing the propagation of situational information in social media during COVID-19 epidemic: A case study on Weibo," *IEEE Trans. Computat. Social Syst.*, vol. 7, no. 2, pp. 556–562, Mar. 2020.

[3] X. Liu, L. Zheng, X. Jia, H. Qi, S. Yu, and X. Wang, "Public opinion analysis on novel coronavirus pneumonia and interaction with event evolution in real world," *IEEE Trans. Computat. Social Syst.*, vol. 8, no. 4, pp. 1042–1051, Aug. 2021.

[4] Y. Zhao, J. Huang, L. Zhang, X. Lian, and D. Wang, "Is the omicron variant of SARS-CoV-2 coming to an end?" *Innovation*, vol. 3, no. 3, May 2022, Art. no. 100240.

[5] S. L. Chang, N. Harding, C. Zachreson, O. M. Cliff, and M. Prokopenko, "Modelling transmission and control of the COVID-19 pandemic in Australia," *Nature Commun.*, vol. 11, no. 1, pp. 1–13, Nov. 2020.

[6] G. Giordano *et al.*, "Modelling the COVID-19 epidemic and implementation of population-wide interventions in Italy," *Nature Med.*, vol. 26, no. 6, pp. 855–860, Apr. 2020.

[7] N. Gozzi, M. Tizzoni, M. Chinazzi, L. Ferres, A. Vespignani, and N. Perra, "Estimating the effect of social inequalities on the mitigation of COVID-19 across communities in Santiago de Chile," *Nature Commun.*, vol. 12, no. 1, pp. 1–9, Apr. 2021.

[8] W. Zhang *et al.*, "Dynamic-fusion-based federated learning for COVID-19 detection," *IEEE Internet Things J.*, vol. 8, no. 21, pp. 15884–15891, Nov. 2021.

[9] R. Wang, C. Ji, Z. Jiang, Y. Wu, L. Yin, and Y. Li, "A short-term prediction model at the early stage of the COVID-19 pandemic based on multisource urban data," *IEEE Trans. Computat. Social Syst.*, vol. 8, no. 4, pp. 938–945, Aug. 2021.

[10] G. Rozhnova *et al.*, "Model-based evaluation of school-and non-school-related measures to control the COVID-19 pandemic," *Nature Commun.*, vol. 12, no. 1, pp. 1–11, Mar. 2021.

[11] E. Ramírez-Llanos and S. Martínez, "A distributed dynamics for virus-spread control," *Automatica*, vol. 76, pp. 41–48, Dec. 2016.

[12] J. Xue, M. Zhang, and M. Xu, "Modeling the impact of social distancing on the COVID-19 pandemic in a low transmission setting," *IEEE Trans. Computat. Social Syst.*, early access, Dec. 1, 2021, doi: 10.1109/TCSS.2021.3129309.

[13] F.-Y. Wang, "Toward a paradigm shift in social computing: The ACP approach," *IEEE Intell. Syst.*, vol. 22, no. 5, pp. 65–67, Sep. 2007.

[14] V. Marjanović, M. Milovančević, and I. Mladenović, "Prediction of GDP growth rate based on carbon dioxide (CO_2) emissions," *J. CO_2 Utilization*, vol. 16, pp. 212–217, Dec. 2016.

[15] R. Zhang, Y. Zhang, H. Lin, X. Feng, T.-M. Fu, and Y. Wang, "NOx emission reduction and recovery during COVID-19 in east China," *Atmosphere*, vol. 11, no. 4, p. 433, Apr. 2020.

[16] B. Zheng *et al.*, "Satellite-based estimates of decline and rebound in China's Co_2 emissions during COVID-19 pandemic," *Sci. Adv.*, vol. 6, no. 49, Dec. 2020, Art. no. eabd4998.

[17] Z. Liu *et al.*, "Near-real-time monitoring of global Co_2 emissions reveals the effects of the COVID-19 pandemic," *Nature Commun.*, vol. 11, no. 1, pp. 1–12, Oct. 2020.

[18] R. Wang *et al.*, "Daily CO_2 emission reduction indicates the control of activities to contain COVID-19 in China," *Innovation*, vol. 1, no. 3, Nov. 2020, Art. no. 100062.

[19] X. Lu *et al.*, "Mobile phone-based population flow data for the COVID-19 outbreak in mainland China," *Health Data Sci.*, vol. 2021, Jun. 2021, Art. no. 9796431.

[20] S. Tan *et al.*, "Mobility in China, 2020: A tale of four phases," *Nat. Sci. Rev.*, vol. 8, no. 11, Aug. 2021, Art. no. nwab148.

[21] Z. Zhu *et al.*, "Strategy evaluation and optimization with an artificial society toward a Pareto optimum," *Innovation*, vol. 3, no. 5, Sep. 2022, Art. no. 100274.

[22] H. Chen *et al.*, "Evaluating the mitigation strategies of COVID-19 by the application of the CO_2 emission data through high-resolution agent-based computational experiments," *Environ. Res.*, vol. 204, Mar. 2022, Art. no. 112077.

[23] W. Duan *et al.*, "An ACP approach to public health emergency management: Using a campus outbreak of H1N1 influenza as a case study," *IEEE Trans. Syst., Man, Cybern. Syst.*, vol. 43, no. 5, pp. 1028–1041, Sep. 2013.

[24] Y. Ge, L. Liu, X. Qiu, H. Song, Y. Wang, and K. Huang, "A framework of multilayer social networks for communication behavior with agent-based modeling," *Simulation*, vol. 89, no. 7, pp. 810–828, Mar. 2013.

[25] Y. Ge, R. Meng, Z. Cao, X. Qiu, and K. Huang, "Virtual city: An individual-based digital environment for human mobility and interactive behavior," *Simulation*, vol. 90, no. 8, pp. 917–935, May 2014.

[26] E. Golder and J. Settle, "The box-müller method for generating pseudo-random normal deviates," *J. Royal Stat. Soc. C Appl. Statist.*, vol. 25, no. 1, pp. 12–20, 1976.

[27] Q. Nie, Y. Liu, D. Zhang, and H. Jiang, "Dynamical SEIR model with information entropy using COVID-19 as a case study," *IEEE Trans. Computat. Social Syst.*, vol. 8, no. 4, pp. 946–954, Aug. 2021.

[28] N. Mustafa, "Research and statistics: Coronavirus disease (COVID-19)," *Int. J. Syst. Dyn. Appl.*, vol. 10, no. 3, pp. 67–86, Jul. 2021.

[29] J. Fan and J. Pan, "On the convergence rate of the inexact Levenberg–Marquardt method," *J. Ind. Manage. Optim.*, vol. 7, no. 1, p. 199, Feb. 2011.

[30] M. H. Zwietering, I. Jongenburger, F. M. Rombouts, and K. V. Riet, "Modeling of the bacterial growth curve," *Appl. Environ. Microbiol.*, vol. 56, no. 6, pp. 1875–1881, 1990.

[31] H. Nishiura, S. Tsuzuki, B. Yuan, T. Yamaguchi, and Y. Asai, "Transmission dynamics of cholera in Yemen, 2017: A real time forecasting," *Theor. Biol. Med. Model.*, vol. 14, no. 1, pp. 1–8, Jul. 2017.

[32] R. Bürger, G. Chowell, and L. Y. Lara-Díaz, "Measuring differences between phenomenological growth models applied to epidemiology," *Math. Biosci.*, vol. 334, Mar. 2021, Art. no. 108558.

[33] B. Efron and R. J. Tibshirani, *An Introduction to Bootstrap*. Boca Raton, FL, USA: CRC Press, 1994.

[34] Q. Li *et al.*, "Early transmission dynamics in Wuhan, China, of novel coronavirus—Infected pneumonia," *New England J. Med.*, vol. 382, no. 13, pp. 1199–1207, Mar. 2020.

[35] A. J. Kucharski *et al.*, "Early dynamics of transmission and control of COVID-19: A mathematical modelling study," *Lancet Infectious Diseases*, vol. 20, pp. 553–558, May 2020.

[36] Y. Liu, A. A. Gayle, A. Wilder-Smith, and J. Rocklöv, "The reproductive number of COVID-19 is higher compared to SARS coronavirus," *J. Travel Med.*, vol. 27, no. 2, pp. 1–4, Apr. 2020.

[37] M. D. Morris, "Factorial sampling plans for preliminary computational experiments," *Technometrics*, vol. 33, no. 2, pp. 161–174, 1991.

[38] F. Meng, B. Su, E. Thomson, D. Zhou, and P. Zhou, "Measuring China's regional energy and carbon emission efficiency with DEA models: A survey," *Appl. Energy*, vol. 183, pp. 1–21, Sep. 2016.

[39] J. S. Jia, X. Lu, Y. Yuan, G. Xu, J. Jia, and N. A. Christakis, "Population flow drives spatio-temporal distribution of COVID-19 in China," *Nature*, vol. 582, pp. 389–394, Apr. 2020.

[40] A. Andronico *et al.*, "Evaluating the impact of curfews and other measures on SARS-CoV-2 transmission in French Guiana," *Nature Commun.*, vol. 12, no. 1, pp. 1–8, Mar. 2021.

[41] L. Tian *et al.*, "Harnessing peak transmission around symptom onset for non-pharmaceutical intervention and containment of the COVID-19 pandemic," *Nature Commun.*, vol. 12, no. 1, pp. 1–12, Feb. 2021.

Zhengqiu Zhu received the B.E. and M.E. degrees in simulation engineering from the National University of Defense Technology, Changsha, China, in 2016 and 2018, respectively, where he is currently pursuing the Ph.D. degree with the College of Systems Engineering.

He was a Visiting Ph.D. Student with the Research Group of Multi-Scale Networked Systems, University of Amsterdam (UvA), Amsterdam, The Netherlands, from 2020 to 2021. His research interests include mobile crowdsensing, social computing, and simulation.

Chuan Ai received the Ph.D. degree in control science and engineering from the National University of Defense Technology, Changsha, China, in 2021.

His research interests include complex networks, epidemic modeling, information diffusion, agent-based simulation, and multiagent modeling.

Hailiang Chen received the B.E. and M.E. degrees in simulation engineering from the National University of Defense Technology, Changsha, China, in 2019 and 2021, respectively, where he is currently pursuing the Ph.D. degree in control science and engineering.

His research interests include complex networks, artificial society, and emergencies.

Bin Chen received the Ph.D. degree in control science and engineering from the National University of Defense Technology (NUDT), Changsha, China, in 2010.

He is currently an Associate Research Fellow with the College of Systems Engineering, NUDT. His current research focuses on Artificial societies, Computational experiments, Parallel execution (ACP)-based simulation running support, parallel experimental methods, data mining, mobile crowdsensing, and microtask crowdsourcing.

Wei Duan received the Ph.D. degree in control science and engineering from the National University of Defense Technology, Changsha, China, in 2014.

His research interests include complex networks, epidemic modeling, information diffusion, agent-based simulation, and social computing.

Xiaogang Qiu received the Ph.D. degree in control science and engineering from the National University of Defense Technology, Changsha, China, in 1998.

He is currently a Professor with the National University of Defense Technology. His research interests include complex networks, epidemic modeling, information diffusion, agent-based simulation, and multiagent modeling.

Xin Lu received the Ph.D. degree from the Department of Public Health Sciences, Karolinska Institutet, Solna, Sweden, in 2013.

He worked at the Department of Sociology, Stockholm University, Stockholm, Sweden, from 2009 to 2012, and the Institute for Future Studies, Stockholm, in early 2013. His research is multidisciplinarily distributed in the following areas: big data analytics, network-based epidemic modeling of infectious diseases, operational research, and graph algorithms.

Ming He was engaged in information and communication engineering post-doctoral research at Southeast University, Nanjing, China, from 2007 to 2009. His research is multidisciplinarily distributed in the following areas: command and control, multiagent modeling, and simulation.

Zhiming Zhao (Senior Member, IEEE) received the Ph.D. degree in computer science from the University of Amsterdam (UvA), Amsterdam, The Netherlands, in 2004.

He is currently an Assistant Professor with the Group of Multi-Scale Networked Systems (MNS) and the System and Networking Laboratory (SNE), UvA. His research interests include cloud computing, software-defined infrastructure, DevOps, big data management, and blockchain. More details are available at https://staff.fnwi.uva.nl/z.zhao/.

Zhong Liu received the Ph.D. degree in system engineering and mathematics from the National University of Defense Technology, Changsha, China, in 2000.

He is currently a Professor of science and technology with the Information Systems Engineering Laboratory, National University of Defense Technology. He is also the Head of the Science and Technology Innovation Team, Ministry of Education. His main research interests include artificial general intelligence, deep reinforcement learning, and multiagent systems.